

# PHYSICAL REVIEW B

## CONDENSED MATTER

THIRD SERIES, VOLUME 42, NUMBER 7 PART A

1 SEPTEMBER 1990

### Excited-state absorption by $\text{Eu}^{2+}$ in $\text{NaF}$ and $\text{KMgF}_3$

Larry D. Merkle

*Center for Night Vision and Electro-Optics, Ft. Belvoir, Virginia 22060-5677\**  
*and Physics Department, University of Arkansas, Fayetteville, Arkansas 72701*

(Received 16 March 1990)

Excited-state absorption (ESA) has been studied in  $\text{NaF}:\text{Eu}^{2+}$  and  $\text{KMgF}_3:\text{Eu}^{2+}$  using a pump-probe technique in the visible region. The pump fluence dependence of fluorescence and transmission gives evidence of ESA in the ultraviolet. A broad ESA band is observed at wavelengths shorter than about 600 nm in  $\text{NaF}:\text{Eu}$ . Comparison of this result with earlier data on  $\text{KBr}:\text{Eu}$ ,  $\text{KCl}:\text{Eu}$ , and  $\text{NaCl}:\text{Eu}$ , and with published photoconductivity data suggests that the ESA is due to photoionization, despite disagreement with the predictions of an electrostatic model for ionization. In  $\text{KMgF}_3:\text{Eu}$  no ESA is evident in the visible, but strong ESA is observed at the 193-nm pump wavelength.

#### I. INTRODUCTION

Divalent europium as a dopant in transparent solids is of interest as a potential solid-state-laser ion. Its strong, broad absorption bands and allowed, vibronic emission band are attractive for a short-wavelength tunable laser.<sup>1,2</sup> However, strong excited-state absorption (ESA) throughout the visible spectral region prevents laser oscillation in  $\text{CaF}_2:\text{Eu}^{2+}$ .<sup>3</sup> This ESA was attributed to ionization of  $\text{Eu}^{2+}$  to  $\text{Eu}^{3+}$ , an assignment supported by an electrostatic model for photoionization.<sup>4</sup> This model can be used to predict that ESA due to ionization should be shifted well into the ultraviolet for  $\text{Eu}^{2+}$  in alkali halides. However, the onset energy for ESA in  $\text{KBr}:\text{Eu}^{2+}$ ,  $\text{KCl}:\text{Eu}^{2+}$ , and  $\text{NaCl}:\text{Eu}^{2+}$  has recently been observed to be about 3.0–3.5 eV, about 4–5 eV lower than predicted.<sup>5</sup> It was found in that study that a charge-transfer transition, involving the transfer of an electron from a neighboring halogen ion to the excited  $\text{Eu}^{2+}$  ion, could better fit the observed ESA onset energies.

This paper reports the extension of this study to  $\text{NaF}:\text{Eu}^{2+}$ .  $\text{F}^-$  has a smaller ionic radius than  $\text{Cl}^-$  and  $\text{Br}^-$ . As a result, the onset of ESA is predicted to occur at a lower energy in  $\text{NaF}$  than in the other hosts if the transition is due to photoionization of  $\text{Eu}^{2+}$ , but at a higher energy if it is due to charge transfer from the halogen to the europium. Thus, the study of ESA in this host serves as a test of the mechanism. Measurements have also been made on  $\text{KMgF}_3:\text{Eu}^{2+}$ . Due to the small crystalline field at the  $\text{Eu}^{2+}$  site in this material, the metastable state of  $\text{Eu}^{2+}$  belongs to the configuration  $4f^7$ , rather than the  $4f^65d$  metastable state of  $\text{Eu}^{2+}$  in the alkali

halides.<sup>6,7</sup> Thus, ESA, after relaxation to the metastable state, involves different transitions in this host.

The remainder of this paper is organized as follows. The experimental apparatus and technique are reviewed in Sec. II. The data on  $\text{NaF}:\text{Eu}$  are presented in Sec. III, and those on  $\text{KMgF}_3:\text{Eu}$  in Sec. IV. Interpretation of the data is discussed in Sec. V, and conclusions are drawn in Sec. VI.

#### II. EXPERIMENTS

The apparatus used for most of the measurements has been described previously, so that only a few major characteristics need to be given here.<sup>5</sup> The sample is pumped by a Lumonics excimer laser with about an 8-ns pulse duration and probed in a direction orthogonal to the laser beam by a pulsed Xe lamp focused to a spot smaller than the pump. In the experiments on  $\text{NaF}:\text{Eu}$ , the pump wavelength was 350 nm and the pump beam size was about 3.6 mm by 2.0 mm (full width at half maximum). In experiments on  $\text{KMgF}_3:\text{Eu}$ , the pump wavelength was 193 nm and the beam size about 1.5 mm by 1.1 mm. Transmission of the Xe probe beam was detected by a Tracor Northern optical spectrum analyzer with a photodiode array sensitive to wavelengths longer than about 400 nm. The pump-induced change in absorption was determined by taking the difference between absorbance spectra measured with the probe lamp fired after the pump laser and spectra measured with the lamp fired before the laser. In the case of  $\text{NaF}:\text{Eu}$ , fluorescence occurs in the spectral region of the absorption measurements. Thus, prior to the calculation of the absorbance,

the fluorescence signal for the same pump energy was subtracted from each spectrum.

Two sets of ESA measurements were performed using frequency-tripled output from a Q-switched Quantel YAG:Nd laser as the pump. In one set, the change in transmission of a NaF:Eu sample due to 355-nm pumping was probed at 514.5 nm using a Lexel Ar<sup>+</sup> laser. In the other, the transmission change in the visible region of a KCl:Eu sample was measured using a Hamamatsu streak-camera system.

Aggregation of the Eu<sup>2+</sup>-cation vacancy dipoles occurs in europium-doped alkali halides at room temperature, affecting their optical properties. To determine the influence of this aggregation many NaF:Eu samples were annealed at 875–880 °C and quenched to room temperature to break up aggregates. All optical experiments were carried out at room temperature.

The NaF:Eu and KMgF<sub>3</sub>:Eu samples were obtained from the crystal growth facility of Oklahoma State University. A chemical analysis of one NaF:Eu and two KMgF<sub>3</sub>:Eu samples with well-characterized optical absorption spectra was performed by Galbraith Laboratories, and the Eu<sup>2+</sup> concentrations of other samples were estimated by comparison of their optical absorption with these samples. Typical concentrations were  $2 \times 10^{18}$  cm<sup>-3</sup> in NaF:Eu and  $1 \times 10^{20}$  cm<sup>-3</sup> in KMgF<sub>3</sub>:Eu.

### III. NaF:Eu DATA

The absorption spectra of Eu<sup>2+</sup> in both annealed and quenched and unannealed samples of NaF:Eu are presented in Fig. 1. The difference is comparable to that found in other alkali halides doped with Eu<sup>2+</sup> and attributed to the effects of dopant aggregation.<sup>8,9</sup> This indicates that considerable aggregation of the Eu must have occurred in the unannealed sample during the, approximately, 2 y between growth and measurement, and that

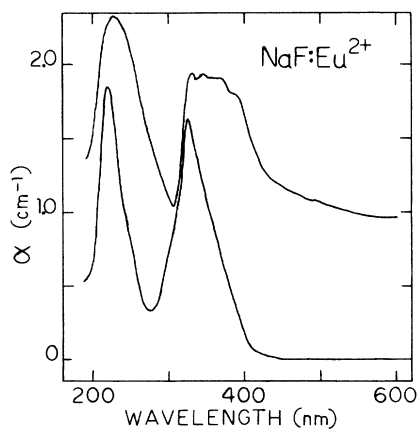


FIG. 1. Absorption spectra of NaF:Eu. Upper trace: absorption of a never-annealed sample (baseline offset for clarity). Lower trace: absorption of a sample annealed at 880 °C for 16 h then quenched to room temperature.

the anneal and quench cycle breaks up (or at least changes) this aggregated state. In support of this conclusion, the unannealed samples appear milky, whereas freshly quenched samples are clear, and remain so for several weeks after quenching.

The fluorescence emitted upon 350-nm laser excitation was found to be so weak in unannealed samples that its spectrum and lifetime could not be measured. In annealed and quenched samples, however, a fairly strong fluorescence was observed with its peak at  $458 \pm 2$  nm and a full width at half maximum of  $71 \pm 2$  nm. The lifetime of this fluorescence is  $1.6 \pm 0.1$   $\mu$ s. This is longer than the temperature-independent lifetime of Eu<sup>2+</sup> in hosts such as KCl.<sup>10</sup> Thus, it appears that, in the heavily aggregated state, the quantum efficiency of Eu<sup>2+</sup> in NaF is near zero, whereas it is significantly higher in annealed and quenched material. The lifetime is found to be the same for anneal times from 16 h to 1 min. The fluorescence strength integrated over time and wavelength was also compared for different annealing times, after scaling for the pump laser energy and the absorption coefficient of the sample at 350 nm. Due to differences in surface quality, only rough trends can be noted. The fluorescence efficiency may be somewhat smaller for samples annealed 30 min or less than for samples annealed for longer times, but is dramatically reduced only for the sample annealed for just 1 min. Thus, it appears that anneal times of even a very few minutes at 880 °C break up the nonfluorescing aggregates almost as effectively as 16-h anneal times. It is not known whether the state achieved by several minutes to 16-h anneal times represents completely isolated Eu<sup>2+</sup> ions, or simply smaller and more durable clusters.

The ground-state absorption cross section at the pump wavelength was estimated based on chemical analysis for Eu in one NaF:Eu sample in which the absorption spectrum after quenching from a 16-h anneal had been measured carefully. The resulting cross section at 350 nm is  $1.04 \times 10^{-18}$  cm<sup>2</sup>. This value was used to infer the Eu<sup>2+</sup> concentration of other annealed and quenched samples from their absorption coefficient.

The integrated fluorescence of an annealed and quenched sample as a function of incident on-axis laser fluence is presented in Fig. 2. The dashed curve is a fit to the data assuming the above value for the ground-state cross section, no ESA or stimulated emission, and adjusting the vertical scale to fit the linear region at low fluence. Clearly the sublinearity in this curve (due to ground-state depletion) is insufficient to fit the data. The solid curve takes ESA of pump photons into account by a model to be discussed in Sec. V.

The transmission of pump light through a 0.19-cm thick annealed and quenched sample has also been measured as a function of incident fluence up to an on-axis fluence of 2.0 J/cm<sup>2</sup>. The transmittance varied only weakly, with a linear fit to the data giving a zero fluence value of 0.605 and a slope of 0.04 cm<sup>2</sup>/J. The scatter in the transmittance values is as large as 0.08, so that the data are consistent with the transmittance being either constant or weakly increasing with fluence.

ESA data in the visible region were taken on several annealed and quenched samples at several pump fluences.

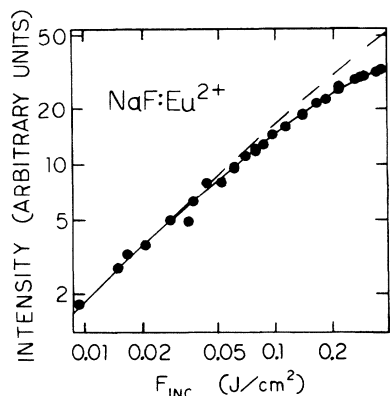


FIG. 2. Pump fluence dependence of the integrated fluorescence from annealed and quenched  $\text{NaF}:\text{Eu}^{2+}$ . The dashed curve is the behavior expected without ESA. The solid curve is that given by the  $\text{NaF}:\text{Eu}$  ESA model discussed in the text with an ESA cross section of  $1.6 \times 10^{-18} \text{ cm}^2$ .

A pump-induced absorption change was observed for wavelengths shorter than about 625 nm. The resulting spectrum for an incident pump energy of 36 mJ and a delay of  $0.5 \mu\text{s}$  between the laser pulse and the peak of the Xe probe pulse is shown in Fig. 3. The different symbols used for data between 425 and 500 nm represent the fact that, in this region, the fluorescence is large enough that a 5% error in subtraction of the fluorescence, the worst-case estimate of this error, would yield a signal-to-error ratio less than one. The absorption change is found to be roughly proportional to the pump energy and to vary with delay time between pump and probe roughly consistent with the  $\text{Eu}^{2+}$  fluorescence lifetime. Thus, the absorption is attributed to ESA by the  $\text{Eu}^{2+}$ .

To verify the ESA a set of experiments on a 0.3-cm thick annealed and quenched  $\text{NaF}:\text{Eu}$  sample was performed using the 514.5-nm output of an  $\text{Ar}^+$  laser as the probe beam, detected by a Si photodiode. With a proper aperture and a long-pass filter, the fluorescence detected by the photodiode could be made sufficiently small so that if the ESA is present a decrease in transmitted signal upon pumping should be observed. Indeed, upon pumping the sample with a 355-nm light at a fluence compara-

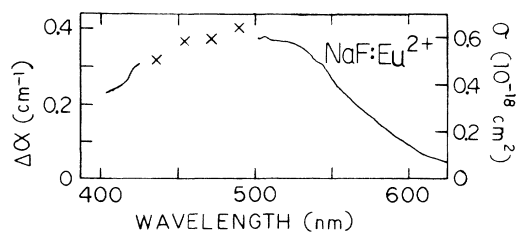


FIG. 3. Excited-state absorption of  $\text{NaF}:\text{Eu}$  in the visible region. The absorption coefficient scale gives the observed absorption change  $0.5 \mu\text{s}$  after the pump pulse for a pump fluence of  $0.28 \text{ J/cm}^2$ . The cross-section scale is that which applies if the  $\text{Eu}^{2+}$  quantum efficiency is one.

ble to those used in the lamp-probed experiments, a 10% decrease in transmission was observed. This decrease recovered with a time constant of  $2.2 \pm 0.5 \mu\text{s}$ , sufficiently close to the fluorescence lifetime to support its identification as ESA from the fluorescing state.

A set of ESA spectra have also been taken in the visible region on a never-annealed sample of  $\text{KCl}:\text{Eu}$ . With an incident on-axis fluence of  $0.75 \text{ J/cm}^2$  and a detection limit of about  $0.02 \text{ cm}^{-1}$ , no pump-induced change in absorption was observed. Using the excited concentration versus pump fluence data in Ref. 5 and assuming a quantum efficiency of unity, the ESA cross section in the visible region must be smaller than  $1.2 \times 10^{-19} \text{ cm}^2$ .

#### IV. $\text{KMgF}_3:\text{Eu}$ DATA

Due to the small crystal-field strength at the  $\text{Eu}^{2+}$  site in  $\text{KMgF}_3:\text{Eu}$ , this material has negligible absorption at 350 nm and therefore was pumped at 193 nm. Comparison of the Eu concentrations with the absorption coefficients of two samples gave an estimated 193-nm ground-state absorption cross section of  $1.27 \times 10^{-19} \text{ cm}^2$ , assuming all Eu to be in the divalent state. In fact, very weak fluorescence lines attributable to  $\text{Eu}^{3+}$  were observed. However, no evidence of  $\text{Eu}^{3+}$  absorption could be found to a detection limit of  $0.025 \text{ cm}^{-1}$ . Based upon the strengths of visible region  $\text{Eu}^{3+}$  transitions in an available stoichiometric  $\text{Eu}^{3+}$  material,  $\text{EuAlO}_3$ , and of the  $4f^7-4f^7$  transitions of  $\text{Eu}^{2+}$  near 360 nm in the  $\text{KMgF}_3:\text{Eu}$  samples, it is estimated that less than 10–15% of the Eu in these samples is in the trivalent state. Thus, the assumption that the total concentration of Eu equals that of  $\text{Eu}^{2+}$  is sufficiently accurate for the present study.

The dominant fluorescence observed upon 193-nm pumping of  $\text{KMgF}_3:\text{Eu}$  is the  $4f^7(^6P)-4f^7(^8S)$  emission near 360 nm. In the present study the lifetime of this fluorescence was found to be 2.8 ms, shorter than the 4.0 ms reported by Altshuler *et al.*<sup>6</sup> This may indicate a modest degree of quenching at room temperature in our samples. The fluorescence signal strength is plotted against the incident on-axis fluence in Fig. 4. Due to the small sample thickness, this signal is a sum over the fluorescence excited by the entire pump beam, so that in fitting the data the beam profile and attenuation in the sample must be taken into account. As the dashed curve indicates, the sublinearity of the data cannot be explained by ground-state depletion alone, suggesting that ESA may occur at 193 nm.

No ESA was detectable in the visible region by the pump-probe apparatus for any probe delay time. The detection limit was about  $1 \text{ cm}^{-1}$ . Using the fluorescence data of Fig. 4 and assuming that all the excited Eu ions decay with the observed fluorescence lifetime, the ESA cross section in the visible is estimated to be smaller than  $5 \times 10^{-19} \text{ cm}^2$ .

The transmission of pump laser light as a function of incident fluence has also been measured for two  $\text{KMgF}_3:\text{Eu}$  samples. These measurements were made using the reflection from three uncoated optics to attenuate the transmitted beam to protect the detector from dam-

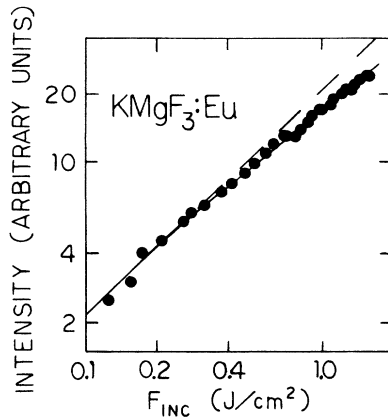


FIG. 4. Pump fluence dependence of the fluorescence from a  $\text{KMgF}_3\text{:Eu}$  sample 0.020-cm thick with a Eu concentration of  $1.2 \times 10^{20} \text{ cm}^{-3}$ . The dashed curve is the behavior expected without ESA. The solid curve is that given by the  $\text{KMgF}_3\text{:Eu}$  ESA model discussed in the text with an ESA cross section of  $2.0 \times 10^{-17} \text{ cm}^2$ .

age. Since this required considerable space between sample and detector, small angle scattering by the sample reduced the apparent transmission. To correct for this a constant has been subtracted from the absorbance data on each sample to make them consistent with very low-intensity data taken with the detector immediately behind the sample. The results are given in Fig. 5, and clearly support the conclusion that processes besides ground-state absorption occur at 193 nm.

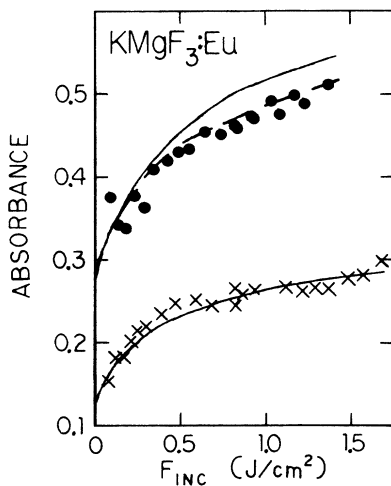


FIG. 5. Pump fluence dependence of the absorbance of two samples of  $\text{KMgF}_3\text{:Eu}$ . Solid circles: sample thickness 0.065 cm and Eu concentration  $7.7 \times 10^{19} \text{ cm}^{-3}$ . Crosses: sample thickness 0.020 cm and Eu concentration  $1.2 \times 10^{20} \text{ cm}^{-3}$ . The parameters which give the solid and dashed curves are discussed in the text.

## V. DISCUSSION

Models involving ESA and various decay modes of the ESA final state have been considered. Numerical fitting of the fluorescence and absorbance data permit tests of these models.

The pump fluence varies with depth in the sample in a way which depends on the ground- and excited-state populations and cross sections. As in an earlier study of ESA in Eu-doped alkali halides, the calculations of depth dependence were carried out in discrete steps, dividing the pump pulse into 50 short segments and the sample beam path into 10 thin slices.<sup>5</sup> Division into smaller steps made little change in the results. The lateral variation in pump fluence was taken into account by approximating each beam with a set of ten regions, each with a constant fluence.

Two simple models are found to fit the fluence dependence of the  $\text{NaF:Eu}$  fluorescence. Each assumes that ESA terminates on a state which decays directly to the ground state rather than the metastable state, such that ESA reduces the efficiency of fluorescence at high fluences, as required to fit the data of Fig. 2. The solid curve in that figure shows the fit achieved by assuming this decay to be so slow that no decay occurs during the pump pulse, and assuming an ESA cross section of  $1.6 \times 10^{-18} \text{ cm}^2$ . A comparably good fit is achieved by a model which assumes this decay to be instantaneously fast, with an ESA cross section of  $1.8 \times 10^{-18} \text{ cm}^2$ .

These two models predict different behaviors for the fluence dependence of the transmission of pump light. If the final state of ESA decays very slowly to the ground state, the excited ion is not available for absorption of additional photons during the laser pulse, since, in these simple models, ESA from this level to still higher states is neglected. Thus, the absorption should bleach as the fluence is increased. By contrast, if that final state decays very rapidly, the absorption bleaches only slightly at modest fluences and grows at higher fluences. Thus, if all the ions in the annealed and quenched sample were in the high-fluorescence quantum efficiency sites, the observed weak increase of absorbance with fluence favors the rapid decay model. However, if many ions remained in sites with nearly zero quantum efficiency even in the freshly quenched sample, the virtually constant absorbance contributed by these ions can make either model consistent with the data. Therefore, parameters for both models are included in Table I, which summarizes the ESA fitting results found in this study.

Using the results of the above calculations, the population of excited ions for a given incident fluence can be found if the fraction of ions in high-quantum-efficiency sites is known. This, in turn, permits the calculation of the ESA cross section in the visible spectral region from the absorption coefficient data of Fig. 3. The cross-section scale given in that figure is that which results if all ions are in high-quantum-efficiency sites. The actual overall quantum efficiency is not known, but in other europium-doped alkali halides it was estimated to be 0.3 or smaller.<sup>5</sup> If the efficiency is less than one in  $\text{NaF:Eu}$  as well, the cross sections in Fig. 3 should be multiplied by

TABLE I. Parameters used in fitting the fluence dependence of fluorescence in  $\text{NaF}:\text{Eu}$  and of fluorescence and absorbance of  $\text{KMgF}_3:\text{Eu}$ . The ground-state-absorption cross section at the pump wavelength,  $\sigma_g$ , and the Eu concentration,  $n_{\text{Eu}}$ , were obtained from the absorption spectra and chemical analysis. Parameters obtained from the fitting are  $\sigma_e$ , the excited-state-absorption cross section at the pump wavelength, RE, the branching fraction for decay of the ESA final state to the metastable state (as opposed to the ground state), and  $\tau$ , the lifetime of the ESA final state.

Sample	$\sigma_g$ ( $\text{cm}^2$ )	$n_{\text{Eu}}$ ( $\text{cm}^{-3}$ )	RE	$\tau$ (ns)	$\sigma_e$ ( $\text{cm}^2$ )
$\text{NaF}:\text{Eu}$	$1.04 \times 10^{-18}$	$1.25 \times 10^{18}$	0	$\gg t_{\text{pump}}$	$1.6 \times 10^{-18}$
$\text{NaF}:\text{Eu}$	$1.04 \times 10^{-18}$	$1.25 \times 10^{18}$	0	0	$1.8 \times 10^{-18}$
$\text{KMgF}_3:\text{Eu}$ (0.020-cm thick sample)	$1.27 \times 10^{-19}$	$1.20 \times 10^{20}$	0.75	5	$2.0 \times 10^{-17}$
$\text{KMgF}_3:\text{Eu}$ (0.065-cm thick sample)	$1.27 \times 10^{-19}$	$7.7 \times 10^{19}$	0.75	16	$2.0 \times 10^{-17}$

the inverse of that efficiency.

The onset energy for the visible ESA transition in  $\text{NaF}:\text{Eu}$  is evidently about 2 eV. This may be compared with the onset energies predicted by electrostatic models for excited-state ionization and halogen-to-europium charge transfer, as has been done for other hosts.<sup>5</sup> The sources of required parameter values are noted in that reference. The resulting onset energies are 4.9–6.1 eV for excited-state ionization, depending on the ligand positions, and roughly 8.5 eV for excited-state charge transfer. Neither agrees with the observed transition, but for the ionization model the variation of onset energy among  $\text{KBr}$ ,  $\text{KCl}$ ,  $\text{NaCl}$ , and  $\text{NaF}$  roughly parallels the data.<sup>5</sup> Since the onset energy is observed to decrease in going from bromide and chloride hosts to the fluoride host, it appears unlikely that charge transfer from the halogen to the Eu is occurring.

A recent report by Aguirre de Carcer *et al.* gives reason to believe that ionization of  $\text{Eu}^{2+}$  in alkali halides may occur at energies as low as those of the ESA band.<sup>11</sup> They observe photoconductivity peaks near 5.5 eV, suggesting excited-state ionization energies of about 2.5 eV. However, the data reported here and in Ref. 5 indicate that the final state of ESA decays to the  $\text{Eu}^{2+}$  ground state, perhaps quite rapidly. Thus, even if the final state of ESA is at host conduction-band energies, it may be that very few electrons excited to that state actually escape. In support of this possibility it has been observed that, although 350-nm laser irradiation induces absorption changes in  $\text{Eu}^{2+}$ -doped alkali halides similar to the effects of ionizing radiation, these changes do not show the fluence dependence expected for excited-state ionization of the Eu.<sup>12</sup>

The ESA onset energy in  $\text{NaF}:\text{Eu}$  is comparable to the  $10Dq$  splitting between the  $4f^65d t_{2g}$  and  $e_g$  states, seen from Fig. 1 to be about 1.7 eV. Thus, an intraionic origin for the ESA cannot be ruled out. However, if this is the case, the visible ESA should also be observable in materials such as  $\text{KCl}:\text{Eu}$ , which has a  $10 Dq$  of about 1.4 eV. No ESA was observed in the visible region in  $\text{KCl}:\text{Eu}$ . The detection limit indicates that if the quantum efficiencies of  $\text{KCl}:\text{Eu}$  and  $\text{NaF}:\text{Eu}$  are equal, any visible ESA in  $\text{KCl}:\text{Eu}$  must be less than one-fifth as strong as in  $\text{NaF}:\text{Eu}$ . Since the fluorescence strength of  $\text{NaF}:\text{Eu}$  is

weaker than that of  $\text{KCl}:\text{Eu}$  for comparable excitation rates, the quantum efficiency of  $\text{NaF}:\text{Eu}$  may well be lower than that of  $\text{KCl}:\text{Eu}$ . If so, the ESA detection limit in  $\text{KCl}:\text{Eu}$  is even more stringent. Thus, transitions within the  $4f^65d$  configuration probably do not account for the  $\text{NaF}:\text{Eu}$  ESA.

In  $\text{KMgF}_3:\text{Eu}$  the available data indicate that ESA is absent or weak in the visible region, but strong at 193 nm. Using the same numerical approach as for  $\text{NaF}:\text{Eu}$  to model the fluence dependence of absorbance and fluorescence data, it is found that no simple model fits all the data. At least some excited ions must bypass the metastable state in their decay from the final state of the ESA transition to explain the sublinearity of the fluorescence data of Fig. 4. Yet, if all decay directly and promptly to the ground state, the observed strong increase in absorbance with fluence is not reproduced. The solid curves in Figs. 4 and 5 were obtained by assuming that the final state of ESA decays to the metastable state with probability 0.75, and with a decay lifetime of 5 ns. The ESA cross section required was  $2.0 \times 10^{-17} \text{ cm}^2$ . The fit to the absorbance data is clearly poorer for the thicker, lower concentration sample, but these data could be fit by assuming a longer lifetime for the decay of the ESA final state, about 16 ns. Processes neglected in the ESA model, such as absorption from the “ESA final state” to still higher states, may also contribute to the imperfect fit. With so many adjustable parameters a unique fit to the data is not possible. Rather, it is concluded that the ESA cross section at the pump laser wavelength must be larger than  $10^{-17} \text{ cm}^2$  and that the decay of the final state probably branches between the metastable state and the ground state.

Lacking data on the ESA spectrum of  $\text{KMgF}_3:\text{Eu}$  between 193 and 400 nm, the onset energy for this transition is unknown. Further, uncertainty as to the position of ligands around the impurity ion results in a wide range of possible onset energies in the ionization model, about 4–10 eV. The only evidence as to the nature of the ESA is its strength, which suggests the large transition dipole moments available in interionic rather than intraionic transitions.

The possibility has been considered that the strong fluence dependence of absorption is due to two-photon

absorption in  $\text{KMgF}_3$ , since its band gap is slightly smaller than twice the 193-nm photon energy.<sup>13</sup> However, the observed fluence dependence corresponds to a two-photon absorption coefficient on the order of 1 cm/MW, about 2 orders of magnitude larger than the largest coefficients reported for any material by Liu *et al.* and 5 orders of magnitude larger than the values typical of materials with band gaps only modestly smaller than twice the photon energy.<sup>14</sup> Thus, excited-state absorption is a much more plausible explanation of the data than two-photon absorption.

## VI. CONCLUSIONS

The similarity of the ESA onset energies of  $\text{NaF:Eu}$  and other Eu-doped alkali halides to the photoconductivity data of Aguirre de Carcer *et al.* suggests that the ESA may indeed be due to ionization.<sup>11</sup> If so, the electrostatic ionization model of Pedrini *et al.* is in error by roughly 4–5 eV, surprising in view of the model's success for alkaline-earth fluorides.<sup>4</sup> Perhaps the final state is more complex than  $\text{Eu}^{3+}$  plus a conduction-band electron. Just as photochromic centers in rare-earth-doped solids are more complex than the simple juxtaposition of a trivalent rare earth and a neighboring  $F$  center,<sup>15</sup> the

final state of the ESA transition may involve the sharing of the electron between the Eu and ligand ions. Clearly more experimental and theoretical work will be required to understand the higher-lying states in these  $\text{Eu}^{2+}$ -doped solids. The nature of the strong ESA in  $\text{KMgF}_3:\text{Eu}$  is even less clear, since only limited data and very uncertain model predictions are available.

The observed excited-state absorption in  $\text{NaF:Eu}$  combined with the earlier data on  $\text{KBr:Eu}$ ,  $\text{KCl:Eu}$ , and  $\text{NaCl:Eu}$ , indicate that alkali halides are not promising hosts for tunable lasers based on  $\text{Eu}^{2+}$ . Although the ESA transitions do not appear to be intraionic, their appearance at much lower energies than predicted by available models indicates that it will be difficult to find a host in which ESA does not interfere with either pumping or stimulated emission.

## ACKNOWLEDGMENTS

The author wishes to thank Professor D. S. McClure for pointing out Ref. 15 and the potential complexity of high-lying excited states of rare-earth ions in solids. He also thanks T. H. Allik, P. K. Bandyopadhyay, and J. A. Hutchinson for their comments and suggestions.

\*Present address.

<sup>1</sup>W. E. Bron and M. Wagner, *Phys. Rev.* **145**, 689 (1966).

<sup>2</sup>G. Blasse, *Phys. Status Solidi B* **55**, K131 (1973).

<sup>3</sup>J. F. Owen, P. B. Dorain, and T. Kobayasi, *J. Appl. Phys.* **52**, 1216 (1981).

<sup>4</sup>C. Pedrini, D. S. McClure, and C. H. Anderson, *J. Chem. Phys.* **70**, 4959 (1979).

<sup>5</sup>L. D. Merkle and P. K. Bandyopadhyay, *Phys. Rev. B* **39**, 6939 (1989).

<sup>6</sup>N. S. Altshuler, L. D. Livanova, and A. L. Stolov, *Opt. Spectrosc.* **36**, 127 (1974) [*Opt. Spectrosc.* **36**, 72 (1974)].

<sup>7</sup>D. K. Sardar, W. A. Sibley, and R. Alcalá, *J. Lumin.* **27**, 401 (1982).

<sup>8</sup>F. J. Lopez, H. Murrieta S., J. Hernandez A., and J. Rubio O., *Phys. Rev. B* **22**, 6428 (1980).

<sup>9</sup>J. Rubio O., H. Murrieta S., J. Hernandez A., and F. J. Lopez, *Phys. Rev. B* **24**, 4847 (1981).

<sup>10</sup>L. D. Merkle, R. C. Powell, and T. M. Wilson, *J. Phys. C* **11**, 3103 (1978).

<sup>11</sup>I. Aguirre de Carcer, F. Cusso, and F. Jaque, *Phys. Rev. B* **38**, 10 812 (1988).

<sup>12</sup>P. K. Bandyopadhyay and L. D. Merkle, *Solid State Commun.* (to be published).

<sup>13</sup>R. R. Daniels, G. Margaritondo, R. A. Heaton, and C. C. Lin, *Phys. Rev. B* **27**, 3878 (1983).

<sup>14</sup>P. Liu, W. L. Smith, H. Lotem, J. H. Bechtel, N. Bloembergen, and R. S. Adhav, *Phys. Rev. B* **17**, 4620 (1978).

<sup>15</sup>D. L. Staebler and S. E. Schnatterly, *Phys. Rev. B* **3**, 516 (1971).